Combust. Sci. Technol., 186: 490–503, 2014

ISSN: 0010-2202 print / 1563-521X online
DOI: 10.1080/00102202.2014.883224

Taylor & Francis
Taylor & Francis Group

DETERMINATION OF LAMINAR BURNING SPEEDS AND MARKSTEIN LENGTHS OF *p*-CYMENE/AIR MIXTURES USING THREE MODELS

Léo Courty,[1] Khaled Chetehouna,[2] Zheng Chen,[3] Fabien Halter,[4] Christine Mounaïm-Rousselle,[4] and Jean-Pierre Garo[5]

[1]*Univ. Orléans, INSA-CVL, PRISME EA 4229, Bourges, France*
[2]*INSA-CVL, Univ. Orléans, PRISME, EA 4229, Bourges, France*
[3]*State Key Laboratory for Turbulence and Complex Systems, Department of Mechanics and Engineering Science, College of Engineering, Peking University, Beijing, China*
[4]*Univ. Orléans, INSA-CVL, PRISME EA 4229, Orléans, France*
[5]*Institut P', CNRS, ENSMA, Univ. Poitiers, Futuroscope Chasseneuil, France*

The aim of this article is to determine the laminar burning speeds and Markstein lengths of* p*-cymene. This fuel is emitted by a typical vegetal species of the Mediterranean region often involved in forest fires. Experiments are performed in a spherical vessel for different equivalence ratios ranging from 0.7 to 1.4 at 180 °C and at atmospheric pressure. The effect of temperature (85 to 180 °C) at the stoichiometry is also studied. Three models (one linear and two nonlinear) are used in the extraction process. Depending on the equivalence ratio, the more accurate models are adopted to determine the laminar burning speeds and Markstein lengths of* p*-cymene. Results are compared favorably to experimental values of a similar fuel (α-pinene) and to numerical data of n-decane computed using the in-house code A-SURF.

Keywords: Laminar flame speed; *p*-Cymene; Stretch

INTRODUCTION

The characterization of vegetation is important in order to accurately model fire propagation because it constitutes the engine of combustion in forest fires. It is widely known that many volatile organic compounds (VOCs) are emitted by vegetal species at different temperatures (Macchioni et al., 2003; Maleknia et al., 2009; Zhao et al., 2009). These VOCs are mostly terpene molecules, and they have very low values of lower flammability limits, namely less than 1% vol. in air (Catoire and Naudet, 2005). Consequently, these compounds are much more flammable than the usual pyrolysis products (CO, C_4H_6, CH_4, etc.). Up to

Received 15 May 2013; revised 24 October 2013; accepted 19 November 2013.
Published as part of the Eighth Mediterranean Combustion Symposium Special Issue with Guest Editors Nevin Selçuk, Federico Beretta, Mohy S. Mansour, and Andrea d'Anna.
Address correspondence to Léo Courty, Univ. Orléans, INSA-CVL, PRISME EA 4229, F-18020, Bourges, France. E-mail: leo.courty@univ-orleans.fr
Color versions of one or more of the figures in the article can be found online at www.tandfonline.com/gcst.

now, VOCs have never been considered in the combustion process of forest fires, and they should be taken into account in the combustion modeling of physical wildland fire models.

Under particular conditions of wind and topography, forest fires can behave in a surprising way, and are characterized by substantial rate of spread and energy released. Such fires are known as accelerating forest fires, and a possible explanation of this phenomenon is the ignition of a VOCs cloud, which is emitted by fire heated vegetation and accumulated in flammable conditions (Barboni et al., 2011; Chetehouna et al., 2009; Courty et al., 2012a). The study of VOCs combustion can be useful to investigate more deeply this hypothesis.

Thymus vulgaris is a well-known aromatic species; it is a typical vegetal fuel of the Mediterranean region often involved in forest fires (Kaloustian et al., 2003). In a recent work, we have performed experiments in a flash pyrolysis apparatus between 70 and 180 °C and found that *p*-cymene is a major compound emitted by this plant (Chetehouna et al., 2012). Thirteen VOCs are emitted by *Thymus vulgaris* needles, and they can be classified into six chemical families according to their molecular formula: monoterpenes ($C_{10}H_{16}$, $C_{10}H_{14}$), sesquiterpenes ($C_{15}H_{24}$), monoterpene phenols ($C_{10}H_{14}O$), monoterpene ethers ($C_{10}H_{18}O$, $C_{10}H_{16}O$), and monoterpene alcohols ($C_{10}H_{18}O$). The percentage of *p*-cymene is between 15% and 30%, and the maximum is reached at about 180°C. It is therefore interesting to investigate the combustion features of this molecule using different models for the extraction of these features from spherical flame experiments.

In the literature, there are very few works studying the combustion of VOCs (Purushotaman and Nagarajan, 2009) and none about the detailed kinetic mechanism of *p*-cymene. Moreover, there are no results on the laminar burning speeds and Markstein lengths of this volatile organic compound. The obtained results will therefore be compared to the experimental values of the major VOC emitted by *Rosmarinus officinalis*, namely α-pinene (Courty et al., 2012b), and to numerical ones of n-decane. Simulations are performed with A-SURF code using the detailed kinetic mechanism of Honnet et al. (2009). Adaptive Simulation of Unsteady Reactive Flow (A-SURF) is a 1D, time-accurate, and space-adaptive numerical solver for initiation and propagation of outwardly propagating spherical flames (Chen, 2010; Chen et al., 2009).

In the next section of this article, the experimental facility is presented and a brief description of the in-house code A-SURF is given. The three different models used for the extraction of combustion characteristics are then presented. The next section is devoted to the results of unstretched flame speeds, Markstein lengths, and laminar burning speeds of *p*-cymene/air mixtures at different equivalence ratios. Experimental results are presented and compared to numerical results of n-decane obtained with A-SURF computational code as well as to experimental results of another VOC available in the literature.

EXPERIMENTAL AND NUMERICAL DESCRIPTION

The laminar burning speed and Markstein length measurements were made using a stainless steel spherical combustion chamber with an inside volume of 4.2 L. Four windows provided optical access into the chamber. Before filling the chamber, vacuum was first created. The amount of gases introduced into the chamber was controlled with a thermal mass flow meter. Synthetic air (79.5% N_2 and 20.5% O_2) was used for the experiments. High purity *p*-cymene ($\geq$ 98% pure from Sigma-Aldrich) was injected through a Coriolis mass flow meter. The mixture was heated up to 180 °C to allow liquids full vaporization, and the chamber minimum temperature was fixed for these experiments at 80 °C to avoid VOCs condensation on the walls inside the chamber. The temperatures chosen to study the effect

of temperature on the laminar burning speed and Markstein length were as follows: 85, 100, 125, 150, and 180°C. The range of equivalence ratio was chosen between 0.7 and 1.4 with a 0.1 step. In these conditions, the amount of fuel injected was totally vaporized. A mixing fan, located inside the chamber, mixed all the gases. Two tungsten electrodes, with a 1 mm gap, connected to a conventional capacitive discharge ignition system, were used to produce spark ignition at the center of the chamber. For each condition, the measurements were repeated three times. The relative error on the equivalence ratio is about 2%, and the uncertainty of unstretched premixed flame is inferior to 5 cm/s.

The flame images were obtained by shadowgraphy. Parallel light was created with a lamp with two plano-convex lenses (25 mm and 1000 mm focal lengths). The shadowgraphic images were recorded using a high speed video CMOS camera (Photron APX) operating at 10,000 frames per second with an exposure time of 20 μs. The temporal evolution of the expanding spherical flame was then analyzed. Figure 1 presents a scheme of the experimental setup, and Figure 2 illustrates the flame front propagation. The luminous circle is an image of the instantaneous flame front: burned gases are inside the circle and unburned ones outside. The images with flame radii less than 7 mm were not analyzed to determine the laminar burning speed and Markstein length, so as to avoid the effect of the initial spark energy deposit (Bradley et al., 1996, 1998; Chen et al., 2009). In order to neglect pressure increase, flame radii larger than 25 mm were not taken into account. In these conditions, the total volume of burned gases is less than 1.6% of the chamber volume.

Numerically, the one-dimensional expanding premixed spherical flame is simulated using the in-house code A-SURF (Chen, 2010; Chen et al., 2009). A-SURF solves the conservation equations for a multispecies reactive flow in one-dimensional spherical coordinate using the finite volume method. The thermodynamic and transport properties as well as the chemical reaction rates are evaluated by CHEMKIN packages (Kee et al., 1989) incorporated into A-SURF. A-SURF has been successfully used in our previous studies on spherical flame initiation and propagation, and the details on the governing equations,

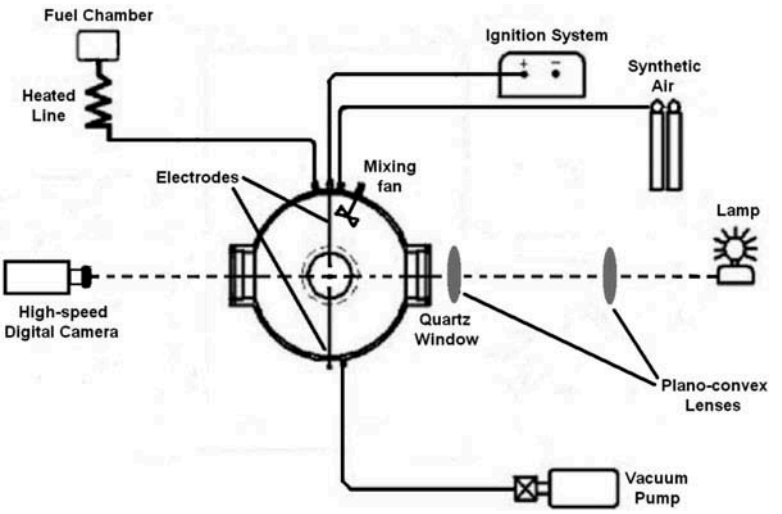

Figure 1 Scheme of the experimental setup.

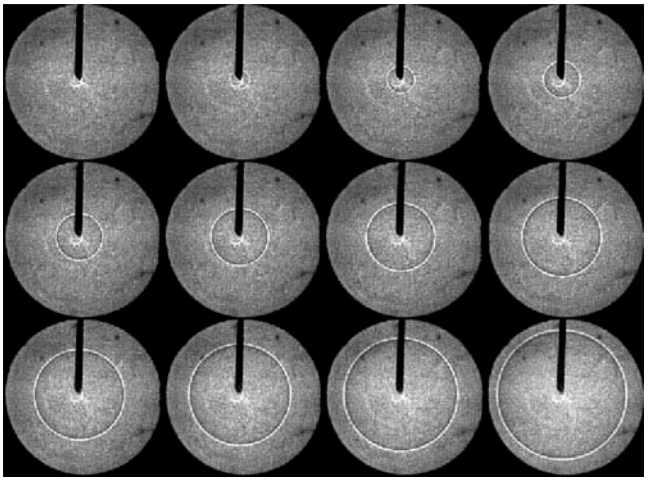

Figure 2 Flame front expansion of a stoichiometric p-cymene/air mixture at 180 °C.

numerical schemes, and code validation can be found in Chen et al. (2009) and Chen (2010). The computational domain is set to be $0 \leq r \leq 50$ cm, and a multilevel, dynamically adaptive mesh is used. The initial and boundary conditions are the same as those used in Chen (2010). The propagating spherical flame is initiated by a small hot pocket (1∼2 mm in radius) of burned product surrounded by fresh mixture at a specified temperature and atmospheric pressure. The size of the hot pocket is chosen so that the effects of ignition can be minimized. In simulation, the flame front, R_f, is defined as the position of maximum heat release and the flame propagating speed is calculated from numerical differentiation, i.e., $S_b = \frac{dR_f}{dt}$.

DIFFERENT MODELS USED IN THE COMBUSTION FEATURES EXTRACTION

In the constant-pressure spherical flame method, the stretched premixed flame speed with respect to burned mixture, $S_b = \frac{dR_f}{dt}$, and the stretch rate, $\kappa = \frac{2S_b}{R_f}$, are obtained from the flame front history, $R_f = R_f(t)$, recorded by high-speed shadowgraph photography. The unstretched laminar flame speed, S_b^0, and Markstein length, L_b, with respect to burned mixture can be extracted based on different models (Chen, 2011). (The laminar burning speed with respect to unburned mixture is $S_u^0 = \sigma S_b^0$, where σ is the expansion factor.) Three extrapolation models can be used in the data processing of the spherical flame method: one is the linear model (LM; the stretched flame speed changes linearly with the stretch rate), and the other two are nonlinear models (NM I and NM II; the stretched flame speed changes nonlinearly with the stretch rate) (Chen, 2011). The expressions for these three models are as follows:

$$\text{LM}: \frac{S_b}{S_b^0} = 1 - \frac{L_b}{S_b^0}\kappa \tag{1}$$

$$\text{NM I}: \frac{S_b}{S_b^0} = 1 - \frac{2L_b}{R_f} \tag{2}$$

$$\text{NM II}: \frac{S_b}{S_b^0}\ln\left(\frac{S_b}{S_b^0}\right) = -\frac{2L_b}{R_f} \tag{3}$$

The LM is well known and popularly used by most of the research groups. The NM I was first proposed by Markstein (1951), and it indicates that the stretched flame speed changes linearly with the curvature. This model was only discussed by Taylor (1991), Karpov et al. (1997), and Chen (2011) and was not used by any other researchers. The NM II was first used by Kelley and Law (2009) and then studied by Halter et al. (2010) and Chen (2011). The NM II was also employed by Tang et al. (2011) in their studies on the laminar flame speed of hydrogen/hydrocarbon blends. It is noted that NM I and NM II are nonlinear only in terms of stretch. In fact, linear extrapolations are conducted based on these two models (based on the plot of S_b versus $2/R_f$ for NM I and that of $\ln S_b$ versus $2/R_f S_b$ for NM II).

It was shown in Chen (2011) that the LM, NM I, and NM II are all accurate to the first-order in terms of the inverse of flame radius, and thus they can be utilized to extract the unstretched laminar burning speed and Markstein length. The accuracy of these models depends on the Lewis number (Chen, 2011). For mixtures with Lewis number appreciably different from unity, both the laminar burning speed and Markstein length are greatly over-predicted from extractions based on the LM. Therefore, in this study, we shall extract the laminar burning speed and Markstein length based on these three models, and comparisons among results from these models will be made and discussed.

RESULTS AND DISCUSSION

Comparison Between Linear and Nonlinear Models

As indicated in the previous section, the three models are used to extract the laminar burning speeds, S_u^0, and Markstein lengths, L_b. The values of S_u^0 are calculated from the relation linking them to the unstretched premixed flame speeds, S_b^0, by means of the expansion factor, σ, $S_u^0 = \sigma \cdot S_b^0$. As mentioned in the Introduction, there are few works in the literature dealing with VOCs combustion (Purushotaman and Nagarajan, 2009) and none about a detailed chemical-kinetic mechanism for *p*-cymene combustion. Consequently, the expansion factor is calculated using the adiabatic flame calculation via the combustion reaction of *p*-cymene with air. Figures 3 and 4 illustrate the evolution of these combustion characteristics as functions of equivalence ratio at 180 °C. It is clear from Figure 3 that the laminar burning speeds evolve as a bell-shape curve as functions of the equivalence ratio. Figure 4 shows that Markstein length is decreasing when equivalence ratio increases, with a decreasing steeper for equivalence ratios higher than 1.2. A similar tendency has been observed by Courty et al. (2012b) for α-pinene/air mixtures.

We can also notice that the obtained values of the laminar burning speeds and Markstein lengths decrease in the order of LM, NM I, and NM II. This is consistent with the theory presented by Chen (2011). The gap between the results of the different models decreases when the equivalence ratio increases, and the values become almost the same at $\varphi = 1.3$ and $\varphi = 1.4$. This is due to the facts that the Lewis number (or Markstein length, as shown in Figure 4) decreases with the equivalence ratio for *p*-cymene/air mixtures and that the difference between results from different models decreases with the Lewis number. The relative gap between the laminar burning speeds obtained with the linear model and

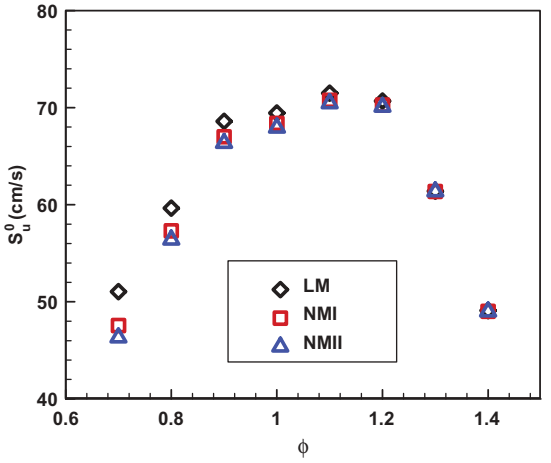

Figure 3 Laminar burning speed as a function of equivalence ratio of *p*-cymene/air mixtures at 180 °C for three models.

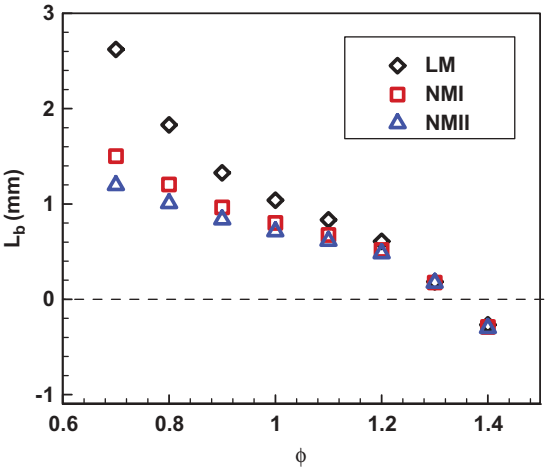

Figure 4 Markstein length as a function of equivalence ratio of *p*-cymene/air mixtures at 180 °C for three models.

the nonlinear models can reach a maximum value of 9% at an equivalence ratio of 0.7. It is obvious from Figure 4 that the discrepancy between the results of the two nonlinear models is lower than the one between linear and nonlinear models for equivalence ratios ranging between 0.7 and 1.2. Indeed, the maximum relative gaps between LM and NM I and between LM and NM II are, respectively, 75% and 118%, whereas the relative gap between NM I and NM II does not exceed 20%. Figure 4 also shows that the Markstein lengths become negative for equivalence ratios higher than 1.3, illustrating the transition between stable and unstable flames.

It has been demonstrated in a previous work (Chen, 2011) that the NM I is more accurate than LM and NM II for mixtures with positive Markstein lengths (large Lewis number), while NM II is the most accurate for mixtures with negative Markstein lengths (small Lewis number). This is illustrated in Figures 5 and 6 for the two equivalence ratios 0.8 and 1.0.

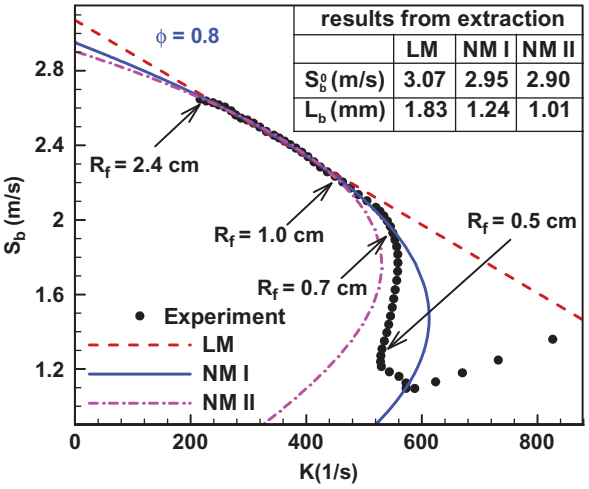

Figure 5 Effects of different models on the extracted flame speed and Markstein length of *p*-cymene/air mixtures at 180 °C at $\varphi = 0.8$.

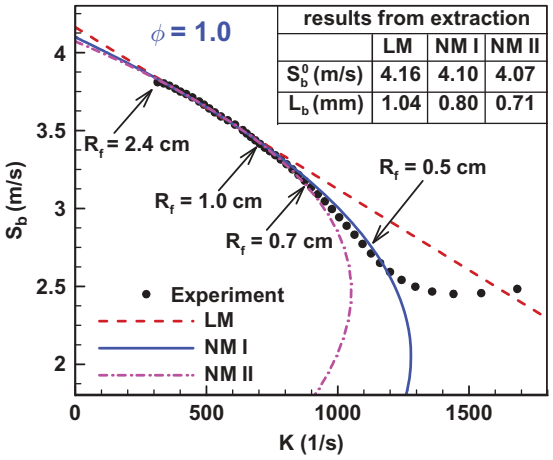

Figure 6 Effects of different models on the extracted flame speed and Markstein length of p-cymene/air mixtures at 180 °C at $\varphi = 1.0$.

Indeed, they present a comparison between the measured stretched flame speeds and those obtained via the three proposed models.

Even if NM II values are close to experimental stretched flame speed for small flame radii (i.e., $0.5 \leq R_f < 0.7$ cm) at $\varphi = 0.8$, NM I is the most accurate for the flame radii range used for extraction (i.e., $0.7 \leq R_f \leq 2.4$ cm) for all equivalence ratios except 1.4. Let us notice that the relative gap between the three models is more important for the extracted Markstein lengths than for the extracted unstretched premixed flame speeds. At the stoichiometry, the relative gap between NM I and NM II is around 1% for S_b^0 and 11% for L_b (respectively 2% and 19% for $\varphi = 0.8$), whereas it is respectively 2% and 30% (respectively 4% and 48% for $\varphi = 0.8$) between LM and NM I.

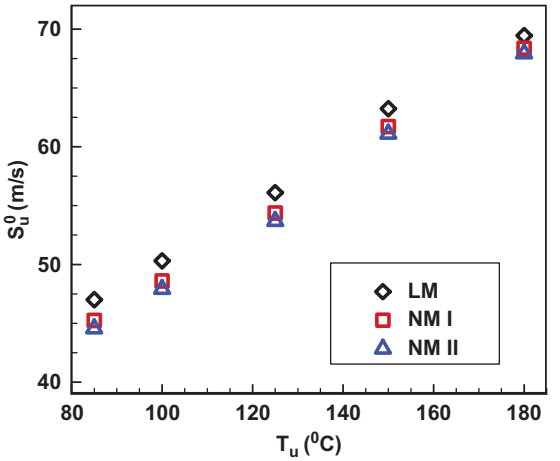

Figure 7 Laminar burning speeds as a function of preheat temperature of *p*-cymene/air mixtures at the stoichiometry for three models.

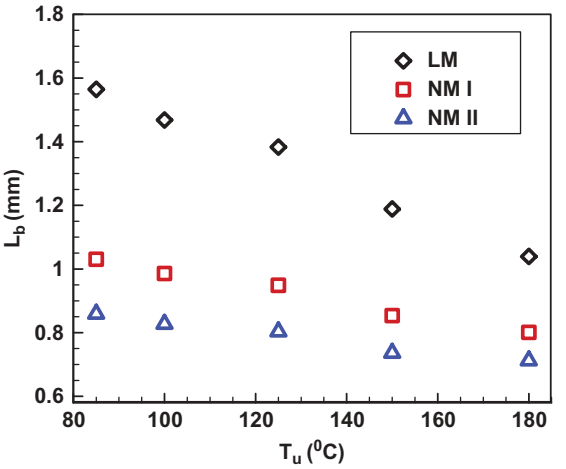

Figure 8 Markstein lengths as a function of preheat temperature of *p*-cymene/air mixtures at the stoichiometry for three models.

When it comes to the preheat temperature effect on the combustion characteristics, Figures 7 and 8 illustrate, respectively, the laminar burning speeds and Markstein lengths obtained using the three models at $\varphi = 1.0$ as functions of temperature. We can observe the same tendency as the one obtained at 180 °C: laminar burning speeds and Markstein lengths values decrease in the order of LM, NM I, and NM II. As indicated above, this result is in agreement with the one given in Chen (2011). The laminar burning speed evolves as a linear function of temperature for the three models used. The relative gap is more important between linear and nonlinear models than between NM I and NM II. Moreover, it decreases with the increase of temperature and can reach maximum values of 5% and 2%, respectively, between LM and nonlinear models and between NM I and NM II at 80 °C.

Concerning the evolution of Markstein lengths as a function of temperature, we can notice that they are always positive and decrease linearly with the increase of temperature for the different models. The decreasing trend is steeper for the linear model than for the two nonlinear models. The relative gap between these models also decreases with the increase of temperature and is higher between linear and nonlinear models than between NM I and NM II. In order to get accurate laminar burning speed and Markstein length from spherical flame experiments, NM I will be used in the next section for *p*-cymene/air mixtures with equivalence ratios lower than 1.3 and NM II for *p*-cymene/air mixtures with $\varphi = 1.4$.

Laminar Burning Speeds and Markstein Lengths

This section presents the laminar burning speeds and Markstein lengths of *p*-cymene/air mixtures obtained using nonlinear models described in the section "Different Models Used in the Combustion Features Extraction." It is noted that in the literature, there are neither available experimental data nor a kinetic mechanism for *p*-cymene. Therefore, we have chosen to compare the present experimental data with measured data of α-pinene (another major VOC emitted by several vegetal species which belongs to the monoterpenoids family, like *p*-cymene) and with computed values of n-decane (which is a molecule with the same number of carbon atoms as *p*-cymene). Figures 9 and 10 illustrate the evolutions of laminar burning speeds and Markstein lengths of *p*-cymene/air mixtures at 180 °C compared to the experimental values of α-pinene/air mixtures (Courty et al., 2012b) and to the numerical ones of n-decane/air mixtures calculated using the in-house code A-SURF and the detailed chemical-kinetic mechanism of Honnet et al. (2009). Indeed, it has been shown by Singh et al. (2010) that the measured laminar burning speeds of n-decane are accurately predicted by this mechanism over most of the range of experiments.

It is clear from Figure 9 that the laminar burning speeds of *p*-cymene are in very good agreement with experimental values of α-pinene for equivalence ratios 0.7 and 0.8 as well as with the numerical ones of n-decane obtained with A-SURF from the stoichiometry to rich mixtures. Let us notice that the three fuels have closed values at the stoichiometry. For

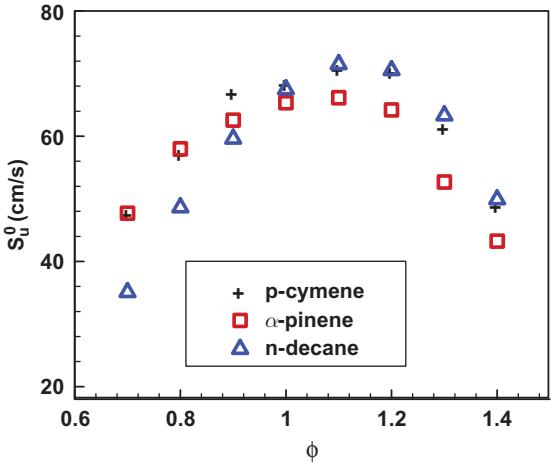

Figure 9 Laminar burning speed as a function of equivalence ratio at 180 °C: results of *p*-cymene/air mixtures (present work), α-pinene/air mixtures (Courty et al., 2012b), n-decane/air mixtures (computed with A-SURF).

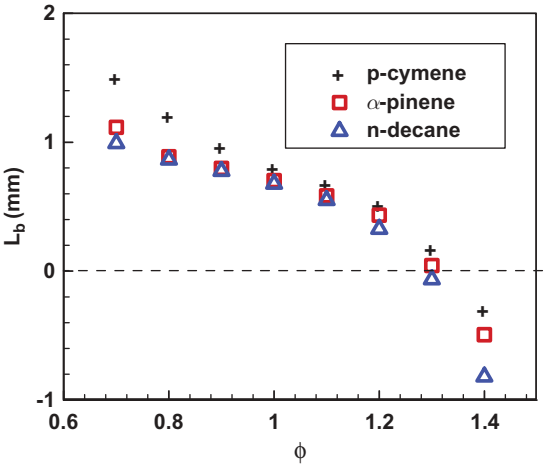

Figure 10 Markstein length as a function of equivalence ratio at 180 °C: results of *p*-cymene/air mixtures (present work), α-pinene/air mixtures (Courty et al., 2012b), n-decane/air mixtures (computed with A-SURF).

equivalence ratios lower than 1, n-decane laminar burning speeds underestimate *p*-cymene values. Measured values of α-pinene underestimate the ones of *p*-cymene for equivalence ratios ranging from 1 to 1.4.

We can see in Figure 10 that the Markstein lengths of *p*-cymene/air mixtures are higher than the experimental data of α-pinene and the numerical ones of n-decane for all equivalence ratios. This might be caused by the different chemistry related to these fuels. n-Decane decomposes more easily into small intermediates and thus it has a relatively smaller effective Lewis number and smaller Markstein length. *p*-Cymene might be more difficult to decompose and hence it has a relatively larger effective Lewis number and larger Markstein length. It is seen that the Markstein lengths of these fuels decrease with the increasing of equivalence ratios, which is consistent with the behavior of heavy hydrocarbon/air flame, in contrast for example to hydrogen/air and methane/air flames. We can also notice that the three hydrocarbons studied here have closed values of Markstein length near the stoichiometry. Indeed, the relative gap between *p*-cymene and the two other fuels does not exceed 20% for equivalence ratios of 0.9, 1.0, and 1.1 and can reach 200% for other equivalence ratios. We can also observe from Figure 10 that the transition between stable and unstable flames occurs around $\varphi = 1.3$ for all these three fuels. This is illustrated by the apparition of cellular instabilities in the temporal evolution of a *p*-cymene/air flame at 180 °C and an equivalence ratio of 1.4, as shown in Figure 11.

After studying the effect of equivalence ratio at 180 °C on the laminar burning speeds and Markstein lengths, it becomes interesting to examine the effect of the preheat temperature at the stoichiometry on these combustion characteristics. Figures 12 and 13 exhibit the evolutions of the laminar burning speed and Markstein length of *p*-cymene/air mixtures as functions of unburned gas temperature at $\varphi = 1.0$ as well as the experimental data of α-pinene/air mixtures and the numerical values of n-decane/air mixtures.

We can see in Figure 12 that the laminar speeds of the three fuels increase when the temperature is increasing. The same tendency has already been observed by Kumar and Sung (2007) for n-decane/air mixtures between 87 and 197 °C and by Tang et al. (2010) for propane/air mixtures between 27 and 167 °C. The laminar burning speeds of *p*-cymene

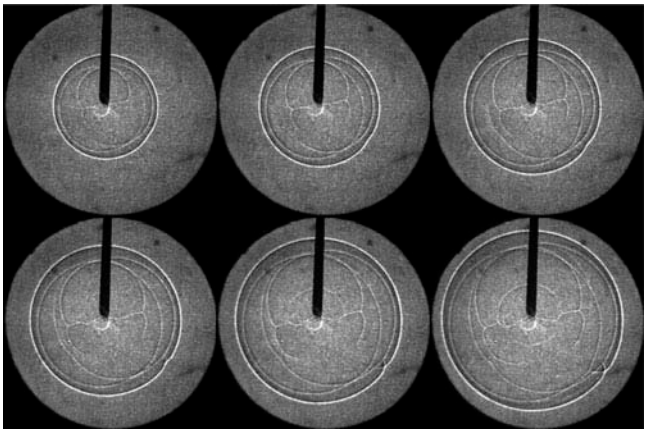

Figure 11 Temporal evolution of a *p*-cymene/air flame at 180 °C and an equivalence ratio of 1.4.

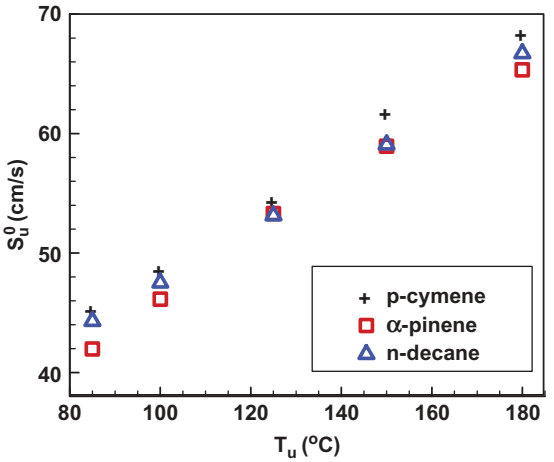

Figure 12 Laminar burning speed as a function of temperature at $\varphi = 1.0$: results of *p*-cymene/air mixtures (present work), α-pinene/air mixtures (Courty et al., 2012b), n-decane/air mixtures (computed with A-SURF).

are higher than the ones of the other fuels for all the studied temperatures and very close to them at 125 °C. The relative deviation between *p*-cymene and n-decane as well as between *p*-cymene and α-pinene has a non-monotonic behavior. It does not exceed 7% between *p*-cymene and α-pinene at 85 °C and 4% between *p*-cymene and n-decane at 150 °C.

Concerning the evolution of Markstein lengths as a function of temperature, Figure 13 shows that they are positive for the three fuels at all temperatures, and the values of *p*-cymene are always higher than the ones of α-pinene and n-decane. As mentioned above, Markstein lengths of *p*-cymene decrease linearly as a function of temperature and we can notice the same behavior for n-decane. Markstein lengths decreasing with the increase of temperature has also been observed by Tang et al. (2010) for propane/air mixtures at the stoichiometry between 27 and 167 °C. This is likely to be caused by the decreasing of flame thicknesses with the increase of the initial temperature. Markstein lengths of α-pinene are

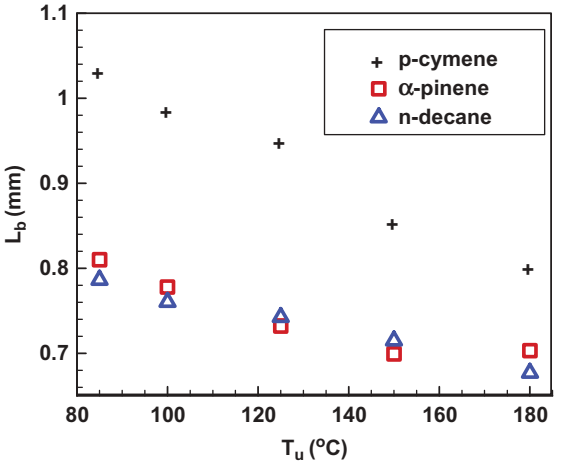

Figure 13 Markstein length as a function of temperature at $\varphi = 1.0$: results of *p*-cymene/air mixtures (present work), α-pinene/air mixtures (Courty et al., 2012b), n-decane/air mixtures (computed with A-SURF).

very close to n-decane values. The relative gap between these two fuels and *p*-cymene decreases with the increase of temperature and varies from 23% to 14%.

CONCLUSION

In the combustion literature, there are few data on the laminar burning speeds and Markstein lengths of volatile organic compounds emitted by vegetal species and none for *p*-cymene. The main purpose of this article is to give its combustion characteristics using the spherical expanding flames methodology and three different models. Among them, we have shown that two nonlinear models are more appropriate to extract the laminar burning speeds and Markstein lengths of *p*-cymene. The laminar burning speeds and Markstein lengths of *p*-cymene/air mixtures at different equivalence ratios and preheat temperatures are obtained. Furthermore, the extracted values of combustion features are compared to the literature experimental data of α-pinene and to the calculated values of n-decane using the A-SURF code, and we have shown that the behavior of *p*-cymene is similar to that of these two fuels. The present study can be useful to consider the combustion of VOCs in the models of physical forest fires and to better understand the phenomenon of accelerating forest fires.

FUNDING

Z. Chen was supported by National Natural Science Foundation of China (Nos. 51322602 and 51136005).

REFERENCES

Barboni, T., Cannac, M., Leoni, E., and Chiaramonti, N. 2011. Emission of biogenic volatile organic compounds involved in eruptive fire, implications for the safety of firefighters. *Int. J. Wildland Fire*, **20**, 152–161.

Bradley, D., Gaskell, P.H., and Gu, X.J. 1996. Burning velocities, Markstein lengths, and flame quenching for spherical methane-air flames: A computational study. *Combust. Flame*, **104**, 176–198.

Bradley, D., Hicks, R.A., Lawes, M., Sheppard, C.G.W., and Woolley, R. 1998. The measurement of laminar burning velocities and Markstein numbers for iso-octane–air and iso-octane–n-heptane–air mixtures at elevated temperatures and pressures in an explosion bomb. *Combust. Flame*, **115**, 126–144.

Catoire, L., and Naudet, V. 2005. Estimation of temperature-dependent lower flammability limit of pure organic compounds in air at atmospheric pressure. *Process Saf. Prog*., **24**, 130–137.

Chen, Z., Burke, M.P., and Ju, Y. 2009. Effects of Lewis number and ignition energy on the determination of laminar flame speed using propagating spherical flames. *Proc. Combust. Inst*., **32**, 1253–1260.

Chen, Z. 2010. Effects of radiation and compression on propagating spherical flames of methane/air mixtures near the lean flammability limit. *Combust. Flame*, **157**, 2267–2276.

Chen, Z. 2011. On the extraction of laminar flame speed and Markstein length from outwardly propagating spherical flames. *Combust. Flame*, **158**, 291–300.

Chetehouna, K., Barboni, T., Zarguili, I., Leoni, E., Simeoni, A., and Fernandez-Pello, A.C. 2009. Investigation on the emission of volatile organic compounds from heated vegetation and their potential to cause an accelerating forest fire. *Combust. Sci. Technol*., **181**, 1273–1288.

Chetehouna, K., Courty, L., Lemée, L., Garo, J.P., and Gillard, P. 2012. Experimental determination of volatile organic compounds emitted by *Thymus vulgaris*. Presented at the 3rd International Conference on Modelling, Monitoring and Management of Forest Fires, New Forest, Royaume-Uni, UK, May 22–24.

Courty, L., Chetehouna, K., Halter, F., Foucher, F., Garo, J.P., and Mounaïm-Rousselle, C. 2012a. Flame speeds of α-pinene/air and limonene/air mixtures involved in accelerating forest fires. *Combust. Sci. Technol*., **184**, 1397–1411.

Courty, L., Chetehouna, K., Halter, F., Foucher, F., Garo, J.P., and Mounaïm-Rousselle, C. 2012b. Experimental determination of emission and laminar burning speeds of α-pinene. *Combust. Flame*, **159**, 1385–1392.

Halter, F., Tahtouh, T., and Mounaïm-Rousselle, C. 2010. Nonlinear effects of stretch on the flame front propagation. *Combust. Flame*, **157**, 1825–1832.

Honnet, S., Seshadri, K., Niemann, U., and Peters, N. (2009) A surrogate fuel for kerosene. *Proc. Combust. Inst*., **32**, 485–492.

Kaloustian, J., El-Moselhy, T.F., and Portugal, H. (2003) Chemical and thermal analysis of the biopolymers in thyme (*Thymus vulgaris*). *Thermochim. Acta*, **401**, 77–86.

Karpov, V.P., Lipatnikov, A.N., and Wolanski, P. 1997. Finding the Markstein number using measurements of expanding spherical laminar flames. *Combust. Flame*, **109**, 436–448.

Kee, R.J., Rupley, F.M., and Miller, J.A. 1989. CHEMKIN-II: A FORTRAN package for the analysis of gas-phase chemical kinetics. Sandia National Laboratory Report, SAND89-8009B.

Kelley, A.P., and Law, C.K. 2009. Nonlinear effects in the extraction of laminar flame speeds from expanding spherical flames. *Combust. Flame*, **156**, 1006–1013.

Kumar, K., and Sung, C.J. 2007. Laminar flame speeds and extinction limits of preheated n-decane/O_2/N_2 and n-dodecane/O_2/N_2 mixtures. *Combust. Flame*, **151**, 209–224.

Macchioni, F., Cioni, P.L., Flamini, G., Morelli, I., Maccioni, S., and Ansaldi, M. 2003. Chemical composition of essential oils from needles, branches and cones of *Pinus pinea, P. halepensis, P. pinaster* and *P. nigra* from central Italy. *Flavour Fragrance J*., **18**, 139–143.

Maleknia, S.D., Vail, T.M., Cody, R.B., Sparkman, D.O., Bell, T.L., and Adams, M.A. 2009. Temperature-dependent release of volatile organic compounds of eucalypts by direct analysis in real time (DART) mass spectrometry. *Rapid Commun. Mass Spectrom*., **23**, 2241–2246.

Markstein, G.H. 1951. Experimental and theoretical studies of flame-front stability. *J. Aeronaut. Sci*., **18**, 199–209.

Purushothaman, K., and Nagarajan, G. 2009. Experimental investigation on a C.I. engine using orange oil and orange oil with DEE. *Fuel*, **88**, 1732–1740.

Singh, D., Nishiie, T., and Qiao, L. 2010. Laminar burning speeds and Markstein length of n-decane/air, jet-A/air and S-8/air flames. Presented at the 48th AIAA Aerospace Sciences Meeting Including the New Horizons Forum and Aerospace Exposition, Orlando, FL, January 4–7.

Tang, C., Huang, Z., and Law, C.K. 2011. Determination, correlation, and mechanistic interpretation of the effects of hydrogen addition on laminar flame speeds of hydrocarbon-air mixtures. *Proc. Combust. Inst*., **33**, 921–928.

Tang, C., Zheng, J., Huang, Z., and Wang, J. 2010. Study on nitrogen diluted propane–air premixed flames at elevated pressures and temperatures. Energy Convers. Manage., **51**, 288–295.

Taylor, S.C. 1991. Burning velocity and the influence of flame stretch. Ph.D. Thesis, University of Leeds.

Zhao, F.J., Shu, L.F., and Wang, Q.H. 2012. Terpenoid emissions from heated needles of *Pinus sylvestris* and their potential influences on forest fires. *Acta Ecol. Sin*., **32**, 33–37.